

ChemComm

Accepted Manuscript



This is an *Accepted Manuscript*, which has been through the Royal Society of Chemistry peer review process and has been accepted for publication.

Accepted Manuscripts are published online shortly after acceptance, before technical editing, formatting and proof reading. Using this free service, authors can make their results available to the community, in citable form, before we publish the edited article. We will replace this *Accepted Manuscript* with the edited and formatted *Advance Article* as soon as it is available.

You can find more information about *Accepted Manuscripts* in the [Information for Authors](#).

Please note that technical editing may introduce minor changes to the text and/or graphics, which may alter content. The journal's standard [Terms & Conditions](#) and the [Ethical guidelines](#) still apply. In no event shall the Royal Society of Chemistry be held responsible for any errors or omissions in this *Accepted Manuscript* or any consequences arising from the use of any information it contains.

COMMUNICATION

Fabrication of Nickel-foam-supported Layered Zinc-Cobalt Hydroxide Nanoflakes for High Electrochemical Performance in Supercapacitors

Cite this: DOI: 10.1039/x0xx00000x

Received 00th January 2012,
Accepted 00th January 2012Peng Yuan,^a Ning Zhang,^{b*} Dan Zhang,^a Tao Liu,^a Limiao Chen,^c Xiaohe Liu,^{a*}
Renzi Ma,^d Guanzhou Qiu^a

DOI: 10.1039/x0xx00000x

www.rsc.org/

Nickel foam supported Zn-Co hydroxide nanoflakes were fabricated by a facile solvothermal method. Benefited from the unique structure of Zn-Co hydroxide nanoflakes on nickel foam substrate, the as prepared material exhibited excellent specific capacitance of 901 F·g⁻¹ at 5 A·g⁻¹ and remarkable cycling stability as electrode material in supercapacitors.

Layered hydroxides are a class of layered materials with metal-hydroxyl host slabs and charge-balancing anions located in interlayers, which has drawn immense attention as functional materials in catalysts,¹ adsorbents,² anion/cation exchangers,³ drug deliverers,⁴ and electrodes.⁵ As an important kind of layered hydroxides, the transition-metal (e. g. Co, Ni) hydroxides possess very desirable electrochemical activity resulted from the good accessibility for redox reactions in supercapacitors (SCs).⁶ Especially, if two transition metals are co-incorporated in the host layer, better capacity and cycling stability are possibly achieved in comparison with monometallic hydroxides. Recently, bimetallic Zn-Co hydroxide, which was composed of divalent zinc and divalent or trivalent cobalt, was widely studied as functional materials. For example, Delorme et al. have studied the synthesis and anion exchange properties of Zn-Co double hydroxide salt;⁷ Woo et al. synthesized the Zn-Co layered hydroxide via a co-precipitation reaction and primarily studied the electrode functionality in SCs;⁸ Zou has reported that Zn-Co layered double hydroxide possessed efficient electro-catalytic property in oxidations of water and alcohol.⁹ Currently, the research about Zn-Co double hydroxide as electrode in SCs is still quite limited. It is highly desirable to explore Zn-Co layered hydroxide materials with good electrochemical performance.

To achieve high energy density for SCs, the electrode materials must possess sufficient surface electro-active species and facilitate the transition of electrons for Faradaic redox reactions.¹⁰ Recently, the Ni foam, which exhibited high electrical conductivity and unique three-dimensional (3D) porous structure, was chosen as the substrate to support the electrode materials to enhance electrochemical performances.¹¹ The Ni foam can provide hierarchical porous channels to ensure efficient contact between the surface of electrode materials and electrolyte,¹² which increase the surface exposed

electro-active species for redox reactions. Furthermore, the direct contact of electrode materials to the conductive Ni foam can not only promote the transition of electrons, but also reduce the “dead volume” produced by a conductive polymer binder additives.¹³ In this regard, to enhance the electrochemical performance for layered Zn-Co hydroxide materials, synthesis of Ni foam-supported Zn-Co hydroxide is a promising method. However, although the growth of layered transition metal hydroxides on Ni foam has drawn a considerable scientific interest (e. g. Ni foam supported Co, Ni, Co-Ni, Co-Al, and Ni-Al hydroxides),¹⁴ there was seldom a report about Ni foam-supported Zn-Co hydroxide. That was because previous methods for synthesizing Zn-Co hydroxide were mainly a rapid co-precipitation reaction in presence of Zn cations, Co cations, and sodium hydroxide,⁷⁻⁹ which usually induced the formation of Zn-Co hydroxide powders rather than the nucleation and growth of Zn-Co hydroxide crystals on the surface of Ni foam. Therefore, in order to generate Ni foam-supported Zn-Co hydroxide materials, it is necessary to develop proper synthetic strategy to slow-down the reaction rate during the co-precipitation process.

In this study, we have developed a facile solvothermal method to synthesize Zn-Co hydroxide on Ni foam. The slow-release of OH⁻ from hexamethylenetetramine (HMT) and surfactant of polyvinylpyrrolidone (PVP) played crucial role in slow-downing the co-precipitation rate of Zn-Co hydroxide solid solutions. Significantly, the vertically aligned growth of pure Zn-Co hydroxide nanoflakes on Ni foam was successfully achieved, which showed high specific capacitance and excellent cycling stability as electrode material in SCs.

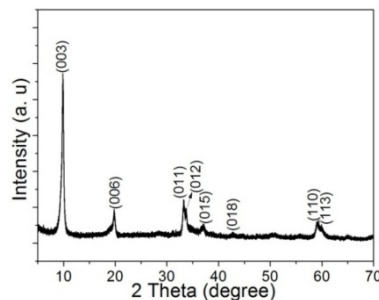


Fig. 1 XRD pattern of as prepared Zn-Co hydroxide.

The experimental process was detailed in ESI†. Firstly, X-ray diffraction (XRD) was used to study the crystal structure of the as prepared product. The powder-like product was obtained from scraping the surface of Ni foam. Fig. 1 shows the XRD pattern of the scraped powder, which indexes to the hydroxalite-like structure (space group: $R\bar{3}m$ (No.166)) and matches well with the previous reports about Zn-Co hydroxide.⁸ A series of {001} Bragg peaks can commonly be observed for the as prepared material, which represent the characteristic peaks of layered α -type hydroxides.¹⁵ There is no other peak observed, indicating that the solid solutions of Zn-Co hydroxide is successfully synthesized. In addition, the distance of layers could be calculated as ~ 0.9 nm according to the Bragg equation. Fourier transform infrared spectroscopy confirmed that CO_3^{2-} and NO_3^- were the main charge-balancing anions located in interlayers of the layered Zn-Co hydroxide (see Fig. S1, ESI†).

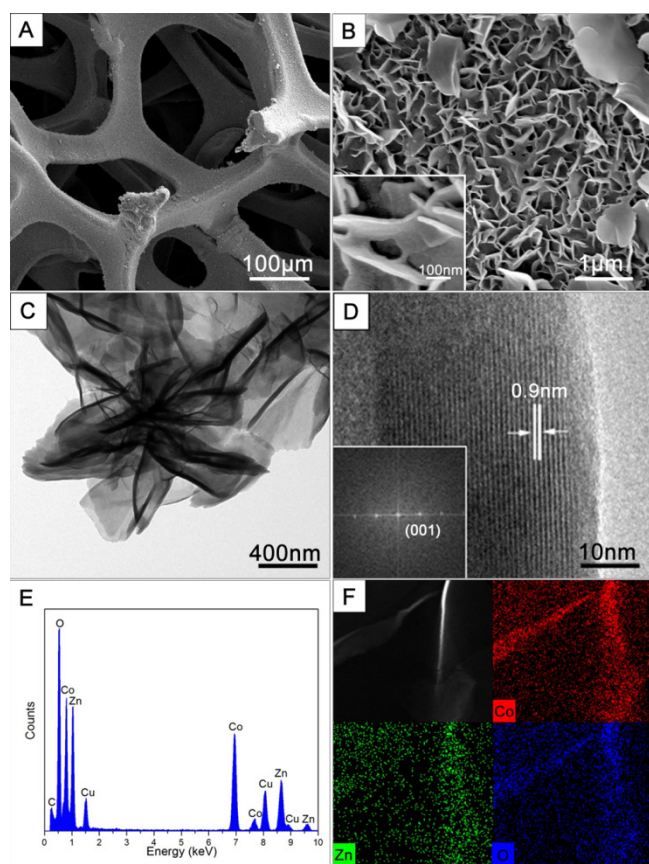


Fig. 2 (A) and (B) SEM images of Zn-Co hydroxide on Ni foam; (C) TEM image, (D) HRTEM image (inset is FFT pattern), (E) EDX spectrum of the Zn-Co hydroxide nanoflakes; (F) STEM image with elemental maps of Co, Zn, and O of the Zn-Co hydroxide nanoflake.

The morphology of the as prepared Zn-Co hydroxide was characterized by scanning electron microscopy (SEM). Fig. 2A shows the SEM image of the Ni foam after the solvothermal process. The coarse surface of Ni foam indicates that the metal Zn-Co hydroxide product was precipitated on the surface. The 3D structure of nickel foam was perfectly kept after the solvothermal process. The SEM in Fig. 2B illustrates that all the precipitated product are nanoflakes. These nanoflakes connected with each other and aligned vertically grow on the nickel foam, which resulted in the formation of resultant porous nanostructure. The higher magnified SEM image in inset of Fig. 2B clearly displays the supported nanoflakes and formed open space between nanoflakes. These nanoflakes possess

average thickness of about 20 nm. Therefore, the ultrathin nanoflakes supported on 3D Ni foam were successfully synthesized. Transmission electron microscopy (TEM) measurements were carried out to further investigate the structure of the as-synthesized Zn-Co hydroxide nanoflakes. In order to efficiently characterize the as prepared Zn-Co hydroxide, the supported materials were carefully scratched from Ni foam. Fig. 2C shows the TEM image of as prepared Zn-Co hydroxide nanoflakes. These nanoflakes connected with each other and formed hierarchical structure. The dark regions are generally the wrinkles of the nanoflakes or junction of the interconnected nanoflakes. The layered structure was also confirmed by HRTEM. Fig. 2D clearly shows the layer distance measured as ~ 0.9 nm, which is identical with the XRD result. The inset in Fig. 2D is the Fast Fourier Transform (FFT) image, which shows the <001> direction for inter-layers of Zn-Co hydroxide. The energy dispersive X-ray spectroscopy (EDX) spectrum in Fig. 2E reveals that the as-obtained product mainly contains Co, Zn, and O elements (C and Cu signals were come from the carbon-supported Cu grid). The Zn:Co ratio was determined to be about 1:2, which was consistent with the ratio of used reagents in synthetic process. Fig. 2F shows a scanning transmission electron microscopy (STEM) image and corresponding elemental maps of Zn-Co hydroxide nanoflake. The elemental maps of Co, Zn, and O match well with STEM image, indicating that these elements are uniformly distributed.

It was reported that the slow-release of OH⁻ from HMT was important for the formation of hydroxide nanoflakes.¹⁶ During the synthesis, the use of HMT is important for the fabrication of Ni foam supported Zn-Co hydroxide. The slow-release effect of HMT not only played important role in the formation of Zn-Co hydroxide nanoflakes, but also could provide enough nucleation and crystallization time for growing on Ni foam surface in solvothermal environment. The direct evidence was that when the HMT was replaced by other alkaline sources (e. g. NaOH or ammonia solutions), the nanoflake-like morphology of Zn-Co hydroxide and growth on Ni foam were difficult to be achieved (see SEM images in Fig. S2, ESI†). On the other hand, the reaction temperature is an important factor in the formation of Zn-Co hydroxide on Ni foam. When the experimental temperature was set to 80 °C and kept other synthetic parameters unchanged, there was almost no Zn-Co hydroxide growing on Ni foam (see Fig. S3, ESI†). That was because the hydrolysis of HMT was not active enough for the formation of Zn(OH)₂-Co(OH)₂ solid solutions at low temperature. In addition, too high temperature (such as 120 °C) could cause the impurity of metal oxides. So, the temperature of 100 °C is a relatively proper experimental condition for generating pure Zn(OH)₂-Co(OH)₂ nanoflakes supported by Ni foam.

Furthermore, the PVP was another important factor for the formation of pure phase Zn-Co hydroxide materials. In a control experiment without PVP, the impurity of cobalt hydroxide was formed (see Fig. S4, ESI†), which was due to that the crystallization rate for cobalt hydroxide was too fast to form pure Zn(OH)₂-Co(OH)₂ solid solutions. It was reported that the PVP was usually used as surfactant to reduce the crystalline nucleation and growth rate.¹⁷ With the introduction of PVP, the crystalline nucleation and growth rate of cobalt hydroxide was decreased, and thus provided adequate nucleation and growth time for the formation of Zn(OH)₂-Co(OH)₂ solid solutions. It should be noted that the nanflakes still could be obtained without the addition of PVP (see Fig. S5, ESI†). Therefore, in our synthetic strategy, the PVP mainly influenced on the formation of Zn(OH)₂-Co(OH)₂ solid solutions, but did not have obvious effect on the nanoflake-like morphology.

In the following study, the electrochemical performances of the pure Zn-Co hydroxide were studied. Fig. 3A shows the representative CV curves of Zn-Co hydroxide at scan rates ranged

from 5 to 100 $\text{mV}\cdot\text{s}^{-1}$. The well-defined redox peaks within -0.1-0.55 V appear in all CV curves, which exhibits that the electrochemical capacitance of the Zn-Co hydroxide is derived from pseudocapacitive behavior of reversible Faradaic redox reactions. Two quasi-reversible electron-transfer processes are visible, which is ascribed to two plausible reactions at the electrode/electrolyte interface. The first pair of peaks at about 0~0.1V is due to the conversion between $\text{Co}(\text{OH})_2$ and CoOOH : $\text{Co}(\text{OH})_2 + \text{OH}^- \rightleftharpoons \text{CoOOH} + \text{H}_2\text{O} + \text{e}^-$. The second pair of peaks at about 0.1~0.4V is assigned to the change between CoOOH and CoO_2 : $\text{CoOOH} + \text{OH}^- \rightleftharpoons \text{CoO}_2 + \text{H}_2\text{O} + \text{e}^-$. The content of zinc does not play any role in the electrochemical active sites, but have an effect by promoting the reaction species in accessing the oxidized cobalt ions.⁹ Furthermore, the shape of CV curves is not significantly influenced by the increase of the scan rate. Even at a high scan rate of 100 $\text{mV}\cdot\text{s}^{-1}$, the CV curve still displays clear redox peaks, which suggests that Zn-Co hydroxide supported by Ni foam is beneficial to fast redox reactions.¹⁸ In addition, the increasing scan rate caused the increase of the internal diffusion resistance in the pseudoactive material, which induced the increase of current and the oxidation/reduction peaks shifted to a more positive/negative positions. In the as prepared Ni foam-supported Zn-Co hydroxide electrode, the peak potential shifts only about 80 mV from 5 $\text{mV}\cdot\text{s}^{-1}$ to 100 $\text{mV}\cdot\text{s}^{-1}$, which is much lower than the previous reported hydroxides,^{14d, 19} indicating the low resistance of the electrode as well as the super-fast electronic and ionic transport rate of as prepared Ni foam supported Zn-Co hydroxide electrode. The low resistance could be verified by electrochemical impedance spectroscopy (EIS) measurement (see Fig. S6, ESI†). The chemical formula of the prepared product was determined to be $\text{Co}_{0.67}\text{Zn}_{0.33}(\text{OH})_{1.66}(\text{NO}_3)_{0.22}(\text{CO}_3)_{0.06}\cdot 0.44\text{H}_2\text{O}$ and corresponding theoretical specific capacitance was calculated as $2261 \text{ F}\cdot\text{g}^{-1}$ within 0.5V, as shown in table S1 of ESI†. To evaluate the electrochemical capacitive performance of Zn-Co hydroxide, the galvanostatic charge-discharge (CD) measurements were carried out within the potential window of 0 to 0.5 V at a set of current densities ranging from 5 to 30 $\text{A}\cdot\text{g}^{-1}$. As shown in Fig. 3B, a relatively symmetric shape during the charge-discharge process is observed, indicating the good supercapacitive behaviors. As shown in Fig. 3C, the specific capacitance can be calculated as $901 \text{ F}\cdot\text{g}^{-1}$ (at 5 $\text{A}\cdot\text{g}^{-1}$), $843 \text{ F}\cdot\text{g}^{-1}$ (at 10 $\text{A}\cdot\text{g}^{-1}$), $800 \text{ F}\cdot\text{g}^{-1}$ (at 15 $\text{A}\cdot\text{g}^{-1}$), $758 \text{ F}\cdot\text{g}^{-1}$ (at 20 $\text{A}\cdot\text{g}^{-1}$), $714 \text{ F}\cdot\text{g}^{-1}$ (at 25 $\text{A}\cdot\text{g}^{-1}$), and $671 \text{ F}\cdot\text{g}^{-1}$ (at 30 $\text{A}\cdot\text{g}^{-1}$), respectively. This suggests that about 74.5% of the capacitance is still retained when the charge-discharge rate is increased from 5 to 30 $\text{A}\cdot\text{g}^{-1}$, reflecting the good ion diffusion and electron transport ability at high current density. To the best of our knowledge, such high pseudocapacitive behavior is much better than previous report about Co-Ni, Co-Al, and Ni-Al hydroxides materials.^{14e, 19b, 20} The high performance for Ni foam-supported Zn-Co hydroxide could be attributed to the efficient contact between the surface of electrode materials and electrolyte as well as the fast electron transitions. The overall results showed better electrochemical performances in compared with the previous reports, such as Zn-Co hydroxide film, α - $\text{Co}(\text{OH})_2$ long nanowire arrays/graphite,²¹ Co-Al hydroxides nanosheet/Ni foam,^{14d} and so on^{19a, 20b} (see Table. S2, ESI†), indicating that Zn-Co hydroxides are promising electroactive materials for supercapacitors. In addition, the Ni foam-supported pure Zn-Co hydroxide prepared with PVP showed enhanced electrochemical activity than Ni foam-supported impure Zn-Co hydroxide prepared without PVP (see Fig. S7, ESI†), which was probably ascribed to the better electronic transmissions for pure Zn-Co hydroxide.

To evaluate the electrochemical stability of Zn-Co hydroxide as an electrode material for electrochemical capacitors, CD measurements were carried out for 1000 cycles at the high current

density of 5 $\text{A}\cdot\text{g}^{-1}$ between 0 and 0.5 V. As shown in Fig. 3D, after an activation process for about 1000 cycles, the capacitance value still retains at about 92%, revealing that the Zn-Co hydroxide electrode possesses excellent cycling stability. Remarkably, the Columbic efficiency remains near 100% during the whole cycling test (see Fig. S8, ESI†), suggesting that the charge/discharge processes is highly reversible. The SEM images in Fig. S9 of ESI† show the Zn-Co hydroxide electrode after charging/discharging for 1000 cycles at a current density of 5 $\text{A}\cdot\text{g}^{-1}$. The morphology of the nanoflakes was maintained, which was a good demonstration of the structural stability of Ni foam supported Zn-Co hydroxide.

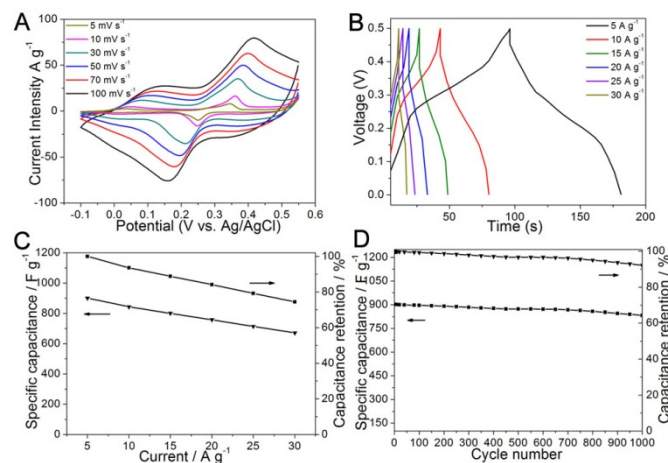


Fig. 3 Electrochemical performances of the Zn-Co hydroxide: (A) CV curves at various scan rates, (B) CD curves at various current densities, (C) the corresponding specific capacitance as a function of current density, and (D) Cycling performance at 5 $\text{A}\cdot\text{g}^{-1}$ for the Ni foam supported Zn-Co hydroxide.

In summary, Ni foam-supported Zn-Co hydroxide nanoflakes were successfully fabricated through a facile solvothermal method. The slow-release effect of HMT and surfactant of PVP played crucial roles in generating the pure phase of Zn-Co hydroxide nanoflakes on Ni foam substrate. During the study of electrochemical performances of the product, the as obtained Ni foam-supported Zn-Co hydroxide nanoflakes exhibited high specific capacitance of $901 \text{ F}\cdot\text{g}^{-1}$ at 5 $\text{A}\cdot\text{g}^{-1}$ and excellent cycling stability. This work provides a promising method to construct Ni foam-supported transition metal hydroxides for the improved electrochemical performance as electrode materials in SCs.

This work is supported by National Natural Science Foundation of China (51372279), Hunan Provincial Natural Science Foundation of China (13JJ1005) and Shenghua Scholar Program of Central South University.

Notes and references

^a School of Resources Processing and Bioengineering, Central South University, Changsha, Hunan 410083, P. R. China.

E-mail: liuxh@csu.edu.cn; Fax: +86 731-8879815

^b School of Materials Science and Engineering, Central South University, Changsha, Hunan 410083, P. R. China

E-mail: nzhang@csu.edu.cn; Fax: +86 731-8879815

^c College of Chemistry and Chemical Engineering, Central South University, Changsha, Hunan 410083, P. R. China.

^d International Center for Materials Nanoarchitectonics (MANA), National Institute for Materials Science (NIMS), Namiki 1-1, Tsukuba, Ibaraki 305-0044, Japan.

† Electronic supplementary information (ESI) available: Experimental procedure and additional figures. See DOI: 10.1039/c000000x/

- 1 S. He, Z. An, M. Wei, D. G. Evans and X. Duan, *Chem. Commun.*, 2013, **49**, 5912.
- 2 X. Y. Yu, T. Luo, Y. Jia, R. X. Xu, C. Gao, Y. X. Zhang, J. H. Liu and X. J. Huang, *Nanoscale*, 2012, **4**, 3466.
- 3 M. Ogawa and K. Kuroda, *Chem. Rev.*, 1995, **95**, 399.
- 4 M. Shao, M. Wei, D. G. Evans and X. Duan, *Chemistry*, 2013, **19**, 4100.
- 5 X. Liu, R. Ma, Y. Bando and T. Sasaki, *Adv. Mater.*, 2012, **24**, 2148.
- 6 (a) H. Du, L. Jiao, K. Cao, Y. Wang and H. Yuan, *Acs Appl. Mater. Interfaces*, 2013, **5**, 6643; (b) G. Chen, S. S. Liaw, B. Li, Y. Xu, M. Dunwell, S. Deng, H. Fan and H. Luo, *J. Power Sources*, 2014, **251**, 338; (c) C. Mondal, M. Ganguly, P. K. Manna, S. M. Yusuf and T. Pal, *Langmuir*, 2013, **29**, 9179.
- 7 F. Delorme, A. Seron, F. Giovannelli, C. Beny, V. Jean-Prost and D. Martineau, *Solid State Ionics*, 2011, **187**, 93.
- 8 M. A. Woo, M. S. Song, T. W. Kim, I. Y. Kim, J. Y. Ju, Y. S. Lee, S. J. Kim, J. H. Choy and S. J. Hwang, *J. Mater. Chem.*, 2011, **21**, 4286.
- 9 X. Zou, A. Goswami and T. Asefa, *J. Am. Chem. Soc.*, 2013, **135**, 17242.
- 10 L. Ren, K. S. Hui and K. N. Hui, *J. Mater. Chem. A*, 2013, **1**, 5689.
- 11 (a) L. Yu, G. Zhang, C. Yuan and X. W. Lou, *Chem. Commun.*, 2013, **49**, 137; (b) M. Kundu, C. C. Ng, D. Y. Petrovykh and L. Liu, *Chem. Commun.*, 2013, **49**, 8459; (c) H. Wang, G. Wang, Y. Ling, F. Qian, Y. Song, X. Lu, S. Chen, Y. Tong and Y. Li, *Nanoscale*, 2013, **5**, 10283.
- 12 C. Yuan, L. Yang, L. Hou, L. Shen, X. Zhang and X. W. Lou, *Energy Environ. Sci.*, 2012, **5**, 7883.
- 13 G. Zhang and X. W. Lou, *Adv. Mater.*, 2013, **25**, 976.
- 14 (a) L. B. Kong, M. C. Liu, J. W. Lang, M. Liu, Y. C. Luo and L. Kang, *J. Solid State Electrochem.*, 2010, **15**, 571; (b) B. Hu, X. Qin, A. M. Asiri, K. A. Alamry, A. O. Al-Youbi and X. Sun, *Electrochim. Acta*, 2013, **107**, 339; (c) H. Chen, L. Hu, M. Chen, Y. Yan and L. Wu, *Adv. Funct. Mater.*, 2014, **24**, 934; (d) Z. Lu, W. Zhu, X. Lei, G. R. Williams, D. O'Hare, Z. Chang, X. Sun and X. Duan, *Nanoscale*, 2012, **4**, 3640; (e) B. Wang, Q. Liu, Z. Qian, X. Zhang, J. Wang, Z. Li, H. Yan, Z. Gao, F. Zhao and L. Liu, *J. Power Sources*, 2014, **246**, 747.
- 15 P. V. Kamath, G. H. A. Therese and J. Gopalakrishnan, *J. Solid State Chem.*, 1997, **128**, 38.
- 16 Z. Liu, R. Ma, M. Osada, K. Takada and T. Sasaki, *J. Am. Chem. Soc.*, 2005, **127**, 13869.
- 17 (a) G. A. Ilevbare, H. Liu, K. J. Edgar and L. S. Taylor, *Cryst. Growth Des.*, 2012, **12**, 3133; (b) U. S. Kestur and L. S. Taylor, *Cryst. Growth Des.*, 2013, **13**, 4349.
- 18 F. Bao, X. Wang, X. Zhao, Y. Wang, Y. Ji, H. Zhang and X. Liu, *RSC Advances*, 2014, **4**, 2393.
- 19 (a) J. Wang, Y. Song, Z. Li, Q. Liu, J. Zhou, X. Jing, M. Zhang and Z. Jiang, *Energ. Fuel*, 2010, **24**, 6463; (b) J. Pu, Y. Tong, S. Wang, E. Sheng and Z. Wang, *J. Power Sources*, 2014, **250**, 250; (c) J. Xu, Y. Dong, J. Cao, B. Guo, W. Wang and Z. Chen, *Electrochim. Acta*, 2013, **114**, 76.
- 20 (a) X. Liu, J. Huang, X. Wei, C. Yuan, T. Liu, D. Cao, J. Yin and G. Wang, *J. Power Sources*, 2013, **240**, 338; (b) J. P. Cheng, J. H. Fang, M. Li, W. F. Zhang, F. Liu and X. B. Zhang, *Electrochim. Acta*, 2013, **114**, 68.
- 21 J. Jiang, J. Liu, R. Ding, J. Zhu, Y. Li, A. Hu, X. Li and X. Huang, *ACS Appl. Mater. Interfaces*, 2011, **3**, 99.